Atomic vibrations in thin $(GaAs)_n(AlAs)_n$ superlattices

K. Lambert and G. P. Srivastava
Department of Physics, University of Exeter, Stocker Road, Exeter, EX4 4QL, United Kingdom
(Received 1 July 1997)

We present theoretical investigations of atomic vibrations in thin $(GaAs)_n(AlAs)_n$ superlattices grown in the favored [001] direction, and also the less well-studied [110] direction, using the *adiabatic bond charge model*. In the acoustic range we confirm the existence of minigaps at the zone center and edges, and also provide evidence for acoustic mode anticrossing and confinement. In the optical range we observe folding, confinement, and mode anisotropy behaviors. The anisotropy is markedly reduced for the [110] system with an angular dispersion opposite to that for the [001] system. The interface mode characteristics are also different for the two growth directions. The highest confined optical mode in the [110] system reaches its bulk value in roughly half the layer width of the [001] system.
[S0163-1829(97)08344-6]

I. INTRODUCTION

Semiconductor superlattices (SL's) have been the subject of many investigations because of their potential applications in devices. While electronic and optical properties of superlattices have been investigated in detail,[1] there have been fewer studies of atomic vibrations. Most studies of atomic vibrations are aimed at the $(GaAs)_m(AlAs)_n$ superlattices grown along [001]. From Raman scattering measurements,[2–8] it has been clearly shown that superlattice formation leads to folded acoustic modes, confined optical modes, and interface modes.

Previous theoretical studies of phonons in semiconductor superlattices, providing support to Raman-scattering measurements, have been made by using both *ab initio* and phenomenological approaches. Molinari, Fasolino, and Kunc[9] used the interplanar force constant method, within the pseudopotential approach and local density-functional approximation, to study superlattice effects on confined phonons. In another *ab initio* study Molinari *et al.*[10] used the *ab initio* pseudopotential approach, within the local-density-functional linear-response theory, to present phonon spectra in ordered and disordered GaAs/AlAs superlattices. On the phenomenological side, Rytov's continuum theory of phonons has been applied[5] to study folded acoustic modes, the linear chain lattice dynamical model has been applied[2] to study longitudinal phonon modes, and full three-dimensional calculations have been made by using the rigid-ion[11–13] and bond charge[14] models. In particular, the works by Molinari *et al.*,[10] Ren, Chu, and Chang,[12] and Chu, Ren, and Chang[13] have provided a detailed account of phonon dispersion, including anisotropy of optical phonons and interface modes, in $(GaAs)_m(AlAs)_n$ [001] SL's.

In this work we use the adiabatic bond charge model, developed for bulk systems by Weber[15] and Rustagi and Weber,[16] to undertake a detailed study of phonon dispersion in $(GaAs)_n(AlAs)_n$ [001] and $(GaAs)_n(AlAs)_n$ [110] superlattices. We examine anticrossing and confinement behaviors in the acoustic range, confinement and anisotropy in the optical range, and GaAs-like as well as AlAs-like interface modes. In addition to agreeing with the theoretical works in Refs. 10, 12, 13, and 14, together with the available Raman-scattering measurements for the [001] SL's, we provide results for [110] SL's.

II. THEORY

Our method of studying phonon dispersion in superlattices uses the adiabatic bond charge model (BCM) developed by Weber[15] for diamond type-structures, and Rustagi and Weber[16] for III-V structures. Such systems are considered with ions and bond charges (BC's) arranged in a tetrahedral arrangement. The model uses six parameters and utilizes five types of short-range interaction: (i) central ion-ion, (ii) central ion-BC, (iii) central BC-BC, (iv) bond-bending ion-BC, and (v) bond-bending BC-BC. The central force interactions just depend on the magnitude of the distance between two particles, while the bond-bending interactions are of the Keating type.[17] In addition to the short-range interactions, long-range Coulombic interactions are considered. These are evaluated by using the Ewald method.[18]

Figure 1 shows the tetrahedral atomic arrangement in the

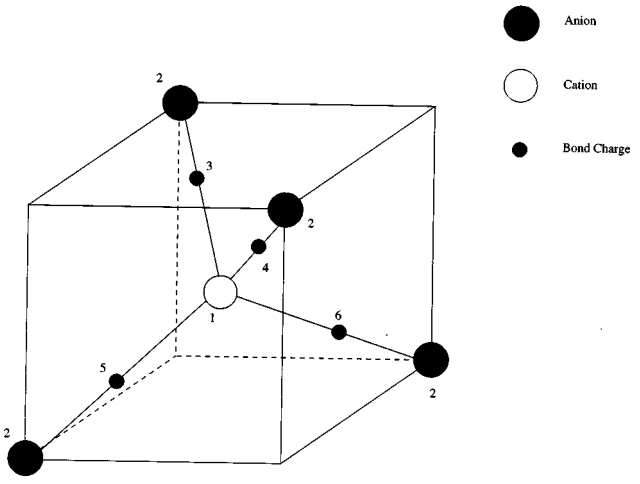

FIG. 1. Diagram showing the tetrahedral coordination of atoms in the zincblende structure. Also indicated are bond charge positions.

material. We considered BC's at the positions of the maximum electronic charge density along the bonds. With reference to Fig. 1, for example, bond charge number 3 is located at the position vector

$$\mathbf{r}_{13}=\frac{(1+p)}{2}\mathbf{r}_{12}, \tag{1}$$

where the ionicity factor is taken as $p=0.25$. The interaction parameters used in this work are taken from Yip and Chang.[14]

Our application of the BCM for SLs differs from that of Yip and Chang.[14] In their work Yip and Chang used complex phonon-dispersion relations for the bulk materials, and used a layer boundary condition to study phonons in SL's. The approach taken needed a perturbation method to include the Coulomb interaction between ionic layers. We used a fully three-dimensional periodic approach, thus not encountering any difficulty with the evaluation of the Coulomb interaction. This three-dimensional periodic approach within the BCM has also been successfully applied in the study of surface phonons on III-V(110) by Tütüncü and Srivastava.[19] In order to deal with arsenic atoms at the interface between the two materials, we used weighted short-range force constants, depending upon how many of the four neighboring bonds are in the respective materials.

The phonon eigenvalues and eigenvectors are calculated by solving the secular equation

$$|C_{\rm tot}(\mathbf{q})-\omega^2\mathbf{I}|=0. \tag{2}$$

In the above, $C_{\rm tot}$ is the total C-type dynamical matrix,[18,19] which can be expressed in terms of the Coulomb and short-range matrices. It should be noted that a three-dimensional periodic approach for phonons in SL's was also used in Refs. 12 and 13. However, these works use the 11-parameter rigid-ion model for bulk semiconductors developed in Ref. 20.

III. RESULTS

We considered $(\mathrm{GaAs})_n(\mathrm{AlAs})_n$ SL's grown along the [001] and [110] directions, with n ranging from 1 to 10. We will denote these as (n,n)[001] and (n,n)[110], respectively. Detailed studies have been made for optical mode confinement and anisotropy, acoustic mode folding, confinement and anticrossing, and optical interface modes. For [001] SL's our results are in agreement with the previous detailed studies by Ren, Chu, and Chang, and by Molinari *et al.*[10,21] To our knowledge, some of the results for the [110] SL's are new.

A. Optical mode folding, confinement, and anisotropy

Phonon states in superlattices can show confinement in the same fashion as electron and hole states.[6,13] Optical modes in each material of a superlattice are subject to boundary conditions similar to those for electron/hole states. In GaAs/AlAs superlattices, we expect AlAs-like LO- as well as TO-phonon modes to be confined, with the difference between the zone-center AlAs and GaAs frequencies creating a well, in analogy with confinement of GaAs hole states. The lack of dispersion of the optical branches for growth direction propagations in Figs. 2(a) and 2(b) confirm this.

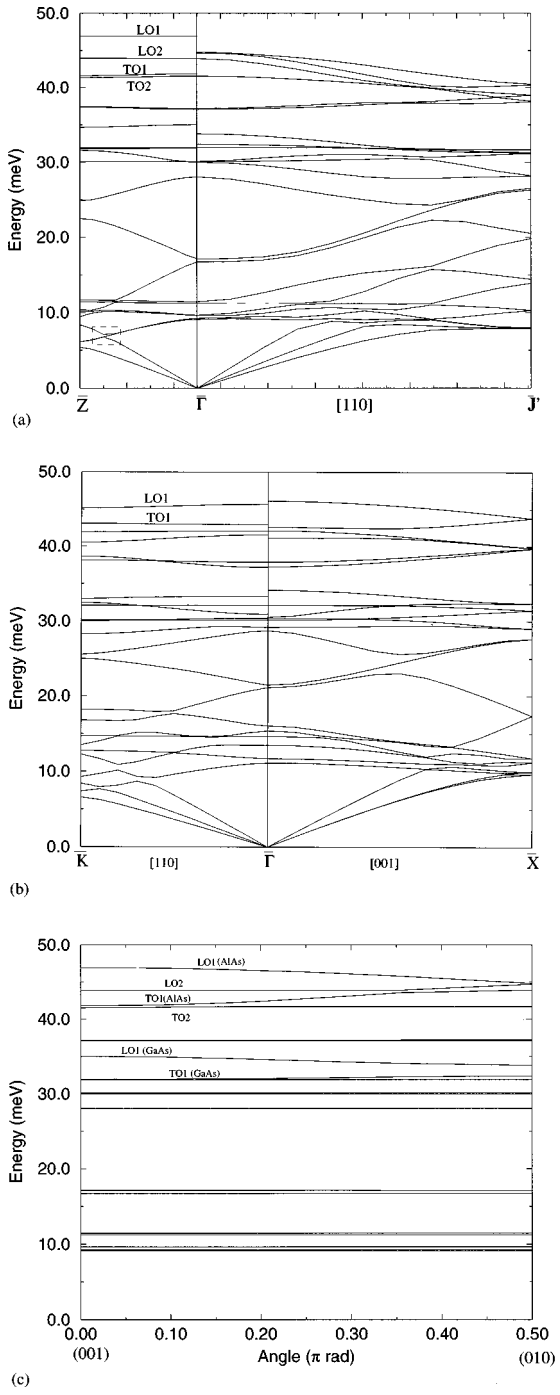

FIG. 2. (a) Phonon-dispersion curves for the $(\mathrm{GaAs})_2(\mathrm{AlAs})_2$ [001] superlattice, displayed in two propagation directions, [001] ($\overline{\Gamma\text{-}Z}$) and [110] ($\overline{\Gamma\text{-}J'}$). We have labeled the AlAs-like LO1, LO2, TO1, and TO2 confined modes. (b) Phonon-dispersion curves for the $(\mathrm{GaAs})_2(\mathrm{AlAs})_2$ [110] superlattice, displayed in two propagation directions, [110] ($\overline{\Gamma\text{-}K}$) and [001] ($\overline{\Gamma\text{-}X'}$). (c) Angular variation of optical-phonon modes for the $(\mathrm{GaAs})_2(\mathrm{AlAs})_2$ [001] superlattice: Phonon energies at a point very close to $\overline{\Gamma}$, with direction varying from [001] to [010] and primary optical modes labelled.

The phenomenon of longitudinal optical phonon anisotropy in the long-wavelength limit for GaAs/AlAs superlattices was first observed in 1980 by Merlin *et al.*,[22] and explained in the detailed theoretical work in Refs. 12 and 13.

The Coulomb force constant matrix between two particles κ and κ' (e.g., ion-ion, ion-BC, BC-BC), in the limit $\mathbf{q}\rightarrow 0$ for a given phonon wave vector $\mathbf{q}$, can be written as[18]

$$C^{Coul}_{\alpha,\beta}(\kappa\kappa'|\mathbf{q}) = A(\kappa,\kappa')\frac{q_\alpha q_\beta}{q^2} + B_{\alpha,\beta}(\kappa,\kappa'|\mathbf{q}), \qquad (3)$$

where A and B are irregular and regular terms, respectively. In the long-wavelength limit the irregular part can be interpreted[18] to arise from the macroscopic electric field due to the presence of dipoles at the atomic sites. For bulk zinc-blende materials the irregular term A is angular independent, and the sum $B+C^{SR}$ (where C^{SR} is the short-range C-type matrix between κ and κ') is rotationally invariant. However, for low-dimensional systems, such as a superlattice, the term A becomes angular dependent, and the sum $B+C^{SR}$ is no longer rotationally invariant. These two factors give rise to the anisotropy in the long-wavelength optical-phonon frequencies.

Figures 2(a) and 2(b) show phonon dispersion for (2,2)[001] and (2,2)[110] SL's along an in-plane direction and along the growth direction. The top two confined AlAs-like LO and TO modes are indicated. We note that the confined AlAs-like LO1 energy is higher than the maximum energy for the corresponding in-plane mode. The anisotropy of the optical modes can be clearly seen from a comparison of the dispersion curves in the limit $\mathbf{q}\rightarrow 0$ from the two directions. As seen in these figures, for in-plane wave vectors both AlAs- and GaAs-like optical modes show ''folding'' effects at the zone edge. It can also be appreciated that there is some evidence of zone folding of (only) the GaAs-like optical modes for wave vectors along the superlattice growth direction. The first unambiguous observation of the latter type of folding was reported in Ref. 3.

The angular dispersion of the anisotropic optical modes in the (2,2)[001] SL can be inspected from Fig. 2(c). As a vanishingly small $\mathbf{q}$ vector changes from the [001] direction to the [010] direction, the highest localized mode (i.e., LO1) disperses downwards in energy. As mentioned earlier, the direction dependence of the optical modes is due to the nonvanishing dipole moment in the geometry applicable. The total dipole moment inside each slab (i.e., material) is approximately proportional to[12]

$$[1-(-1)^n]\cot\frac{n\pi}{2N_s+1},$$

where N_s is the number of bilayers inside each material, and $1\leqslant n\leqslant N_s$ is the index of the confined optical mode. We can see that for a nonvanishing dipole moment n has to be odd, and in addition that $n=1$ has the largest dipole moment. From this we can see that there is only one LO and TO angular-dependent mode per material for the (2,2) superlattice. This is clearly seen for the AlAs-like LO1 , AlAs-like TO1, GaAs-like LO1, and GaAs-like TO1 modes in Fig. 2(c). In addition, we found that, as the layer number increases (toward a more bulk like situation), the modes depicting angular dependence do so in a reduced fashion.

From Fig. 2(b) it can be seen that the energy of the topmost confined mode for the (2,2)[110] SL is somewhat lower than that for the (2,2)[001] SL. In fact, now the AlAs-like LO1 energy lies below the maximum energy of the corresponding in-plane mode. Therefore, as a vanishingly small $\mathbf{q}$ vector changes its direction from [110] to [001], this mode disperses upwards in energy. In other words, the anisotropy of the highest confined mode in the (2,2)[110] SL is of opposite sign to that for the (2,2)[001] SL. We also observe that while this mode is rather flat for the (2,2)[001] SL, it shows a slight dispersion along the growth direction for the (2,2)[110] SL. We expect the difference in the layer stacking configuration in the [001] and [110] SL's to be responsible for these differences: the (110) plane is nonpolar with both cations and anions present, whereas the polar (001) plane has a bilayer.

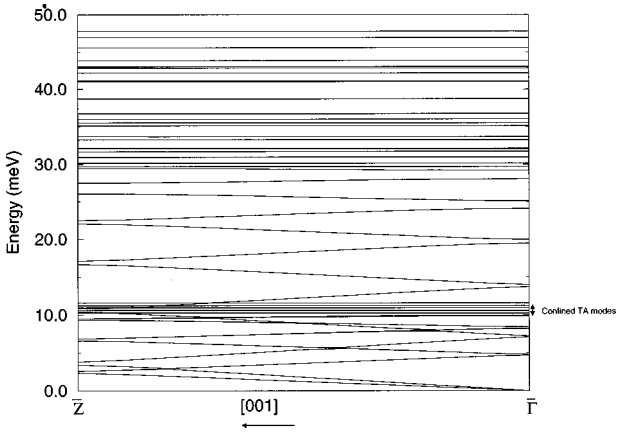

FIG. 3. Phonon-dispersion curve for the $(GaAs)_5(AlAs)_5$ [001] superlattice, showing the confined transverse acoustic modes.

B. Folded and confined acoustic modes

To a first approximation, acoustic modes in a superlattice can be obtained from zone folding the corresponding bulk dispersions in the growth direction. However, in reality superlattice acoustic modes are characterized by confinement, anticrossing, and miniband gaps at the zone center and zone edge. In Fig. 3 we plot the dispersion curve for the (5,5)[001] SL along [001], which clearly shows the zone folding of acoustic modes. Zone-center and zone-edge minigaps in the acoustic range can also be seen in that figure. These minigaps in the acoustic range have also been verified, using Raman-scattering measurements, by Jusserand *et al.*[4]

Also seen in Fig. 3 is the confinement of TA modes in the energy range between the TA edges of GaAs and AlAs, in agreement with the work of Molinari *et al.*[10,21] Analysis of the polarization eigenvectors of these modes shows clearly that the bottom two of these modes are clearly confined to the bulk region of the superlattice and are highly GaAs-like. A confined TA mode is even present in the (1,1) SL, though it is more difficult to attribute this to a confinement process.

Figure 4 illustrates the phenomenon of acoustic mode anticrossing.[1] It shows three GaAs-like modes, taken as a magnification of the part of the diagram indicated by the rectangle in Fig. 2(a) for the (2,2)[001] SL. For the sake of discussion these are labeled TA1, TA2, and LA. One of the degenerate pair modes (TA1) disperses normally, while the other mode (TA2) interacts with the LA mode, and as a result they anticross. A similar acoustic mode anticrossing is also observed in Fig. 2(b) for the (2,2)[110] SL, with the

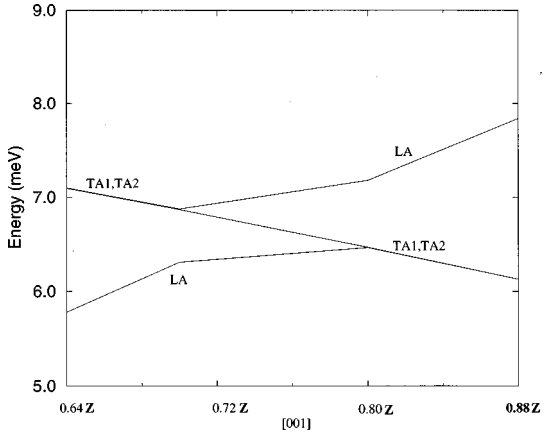

FIG. 4. Magnification of the boxed section of Fig. 2(a) showing anticrossing of acoustic modes for the (2,2) [001] SL.

difference that the TA1 and TA2 modes are no longer degenerate in this case. Occurrence of anticrossing behavior is quite often found in electron states in superlattices.

C. Interface modes

A special feature of superlattice structures is the existence of interface phonon modes. These modes propagate in, and are essentially confined to, the interface layers between the two materials. In Fig. 5(a) we plot the dispersion of the (7,7)[110] SL along the perimeter of the irreducible part of the interface Brillouin zone (i.e., the cross section of the superlattice Brillouin zone at $\mathbf{q}_{[110]}=0$). Also plotted on the same graph are the (110)-projected phonon spectra of bulk GaAs and AlAs.

By inspecting the localization of eigenvectors, we identified four modes shown as two bands of interface states along the $\overline{\Gamma}$ - $\overline{X}$ direction in Fig. 5(b). Each of these pairs is split by up to 1.5 meV at the zone center $\overline{\Gamma}$, but becomes degenerate at the zone edge $\overline{X}$. The upper pair lies in the AlAs optical range and the lower in the GaAs-like optical range. Both these bands are resonant for most of the zone except that the AlAs-like states become truly localized interface states near the zone edge $\overline{X}$, where it lies in the small stomach gap at around 40 meV. This is clearly appreciated from the plots of the eigenvector magnitudes in Fig. 6(a). The polarization characteristics of one of these modes is shown in Fig. 6(b). This corresponds to the TO mode vibration in which the Al atom (labeled 15) in the first AlAs layer vibrates roughly antiparallel to the As atoms (labeled 14 and 18) in the neighboring layers, with components along [110] and [001].

We have also identified a couple of interface vibrational modes for (7,7)[001] superlattices. Our results are in agreement with the theoretical studies of Molinari *et al.*,[10,21] Ren, Chu, and Chang,[12] and Chu, Ren, and Chang,[13] and with the Raman-scattering measurements of Sood *et al.*[7] In particular, at $\overline{J}$ we have identified optical interface modes of AlAs-like character at approximately 38 and 41 meV, and of GaAs-like character at approximately 31 and 32 meV. These can be compared with AlAs-like modes at approximately 44 and 47 meV in the work of Ref. 12, and at 47.5 and 47.6 meV in the work of Molinari *et al.*[10,21] Our GaAs-like results compare well with the Raman-scattering results of 33.2 and 34.45

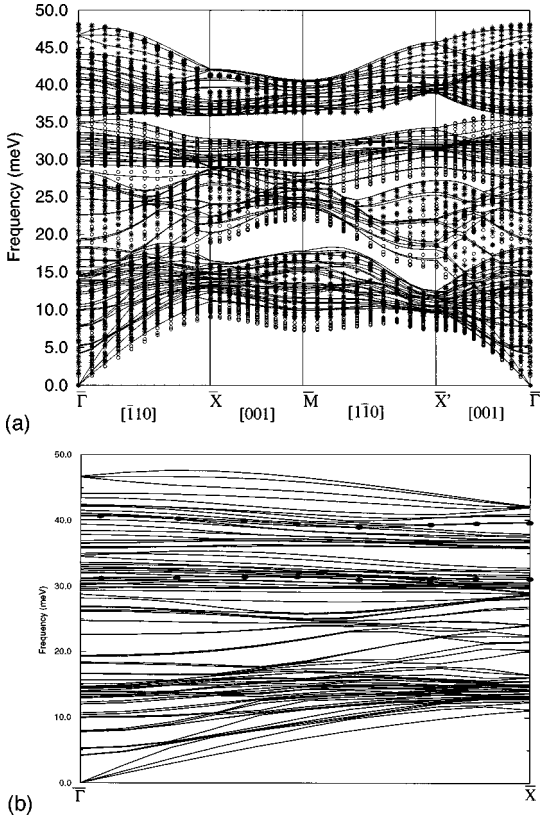

FIG. 5. (a) Phonon-dispersion curves for the $(GaAs)_5(AlAs)_5$ [110] superlattice, shown along the perimeter of the irreducible interface Brillouin zone. The results are overlaid onto a bulk [110] projection, in which the AlAs modes are denoted by asterisks and the GaAs modes by circles. (b) Phonon-dispersion curves for the $(GaAs)_7(AlAs)_7$ [110] superlattice along the $[\overline{1}10]$ direction, with interface modes indicated.

meV obtained by Sood *et al.*[7] A clear indication of interface modes first manifests itself in superlattices as thin as (3,3).

D. Mode tendencies with layer width

In Fig. 7 we plot the dispersion of the AlAs-like LO1, AlAs-like TO1, and GaAs-like LO1 modes as a function of layer thickness. The figure clearly shows a monotonic variation of the LO and TO AlAs-like modes, and the LO GaAs-like modes, toward the bulk values as the layer width increases. Our results for [001] growth direction agree well with the *ab initio* results of Ref. 23 for short-period SL's with $n \leqslant 5$, and also with the Raman scattering measurements in Ref. 24. Also shown in that figure are results of a recent photolumiscence investigation by Litovchenko *et al.*[25] for short-period SL's. While our results for the LO AlAs-like mode agree with the phonon replicas obtained from the photoluminescence spectra for layer thickness index $n \geqslant 4$, there is deviation for $n<4$. The LO GaAs-like modes observed in the photoluminescence spectra, however, lie at appreciably lower energy than our calculated values. This is due to enhanced electron-phonon scattering in the GaAs layer of the Ref. 25 sample.

A noticeable feature of the [110] SL system is that the LO AlAs-like mode attains bulk values for layer thickness index within 10. A comparable layer index number for the LO

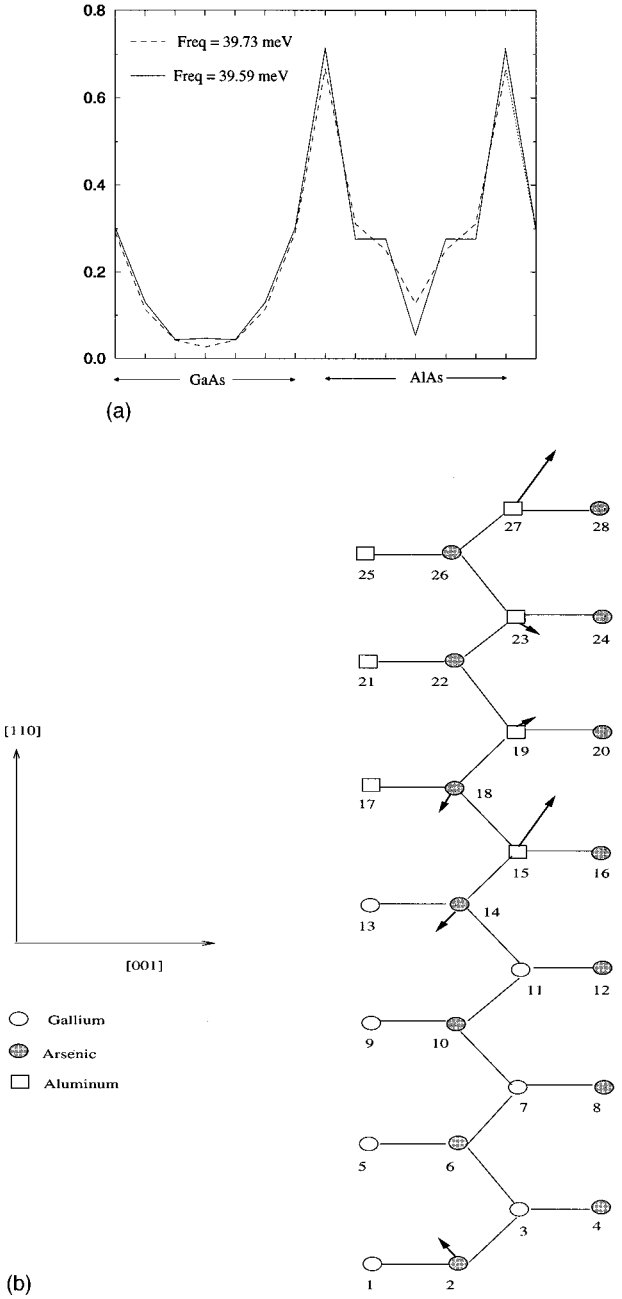

FIG. 6. (a) Magnitudes of atomic polarization vectors for the $(GaAs)_7(AlAs)_7$ [110] superlattice, corresponding to the interface mode at 39.3 meV at the $\overline{X}$point. (b) Schematic of the $(GaAs)_7(AlAs)_7$ [110] superlattice shown in the [110]-[001] plane, together with atomic displacement directions and relative magnitudes for the interface mode discussed in (a).

AlAs-like mode in the [001] system is 15. Taking into account the fact that the width of a layer in the [110] system is $1/\sqrt{2}$ that of one in the [001] system , we can predict that the LO AlAs-like modes in the [110] superlattice will reach the bulk value in approximately half the layer width to that of the [001] case.

IV. SUMMARY

In this paper we used the adiabatic bond-charge model, within a three-dimensional periodic approach, to study the phonon dispersion of [001] and [110] GaAs/AlAs superlattices. We confirmed the existence of mini gaps at the zone center and zone edges in the acoustic range, optical folding, and optical confinement, together with the less intuitive phenomenon of optical mode anisotropy. From a comparison between the [001] and [110] superlattices, we found that the differing geometries and symmetry of the two systems lead to different optical mode anisotropy and different confinement characteristics. The anisotropy is markedly reduced for the [110] system, and is of opposite sign to that for the [001] system.

In addition, we find that the first confined optical mode in the [110] superlattice reaches a bulklike value in roughly half the layer width of the [001] system. We also provided evidence for the existence of acoustic mode anticrossing, and interface modes for the two systems. Again, due to the differing system geometries, the interface mode characteristics are different for the two systems.

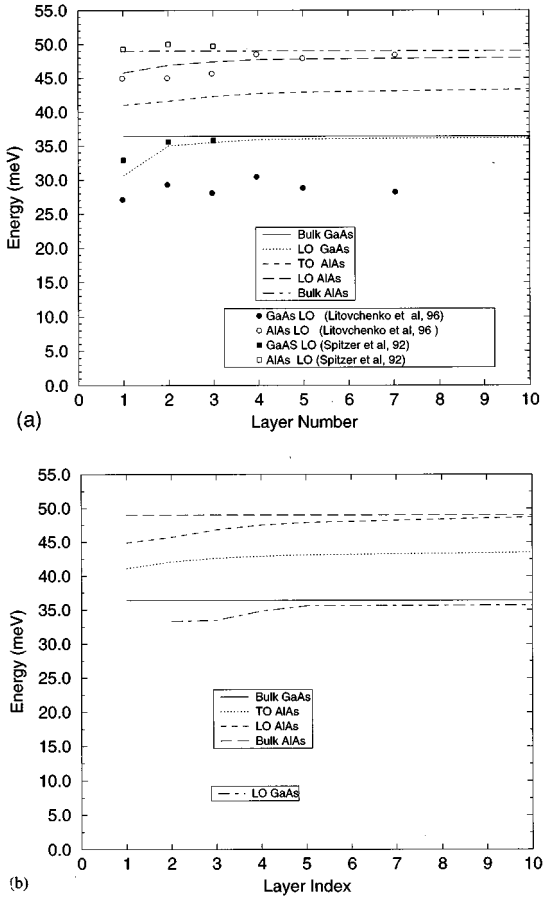

FIG. 7. (a) Variation of AlAs-like LO1, TO1, and GaAs-like LO1 modes, with number n of layers of each material in [001] superlattice. Experimentally detected results are indicated by the various symbols. (b) Variation of AlAs-like LO1 and TO1, and GaAs-like LO1 modes, with number of layers of each material in the [110] superlattice.

ACKNOWLEDGMENT

K. L. wishes to express his thanks to the EPSRC (UK) for financial support.

[1] M. Cardona, Superlattices Microstruct. **7**, 3 (1990).
[2] C. Colvard, T. A. Gant, M. V. Klein, R. Merlin, R. Fischer, H. Morkoc, and A. C. Gossard, Phys. Rev. B **31**, 2080 (1985).
[3] B. Jusserand, D. Paquet, and A. Regrenry, Phys. Rev. B **30**, 6245 (1984).
[4] B. Jusserand, D. Paquet, F. Mollot, F. Alexandre, and G. Le Roux, Phys. Rev. B **35**, 2808 (1987).
[5] B. Jusserand, D. Paquet, and F. Mollot, Phys. Rev. Lett. **63**, 2397 (1989).
[6] B. Jusserand, D. Paquet, F. Alexandre, and A. Regrenry, Surf. Sci. **174**, 94 (1986).
[7] A. K. Sood, J. Menendez, M. Cardona, and K. Ploog, Phys. Rev. Lett. **54**, 111 (1985).
[8] B. Jusserand, F. Alexandre, D. Paquet, and G. Le Roux, Appl. Phys. Lett. **47**, 301 (1985).
[9] E. Molinari, A. Fasolino, and K. Kunc, Superlattices Microstruct. **2**, 397 (1986).
[10] E. Molinari, S. Baroni, P. Gianozzi, and S. de Gironcoli (unpublished).
[11] G. Kanellis, Phys. Rev. B **35**, 746 (1986).
[12] S. F. Ren, H. Chu, and Y. C. Chang, Phys. Rev. B **37**, 8899 (1987).
[13] H. Chu, S. F. Ren, and Y. C. Chang, Phys. Rev. B **37**, 10 746 (1988).
[14] S. Yip and Y. C. Chang, Phys. Rev. B **30**, 7037 (1984).
[15] W. Weber, Phys. Rev. Lett. **33**, 371 (1974).
[16] K. C. Rustagi and W. Weber, Solid State Commun. **18**, 673 (1975).
[17] P. N. Keating, Phys. Rev. **145**, 637 (1966).
[18] A. A. Maradudin *et al.*, *Theory of Lattice Dynamics in the Harmonic Approximation*, 2nd ed. (Academic, New York, 1971).
[19] H. M. Tütüncü and G. P. Srivastava, J. Phys.: Condens. Matter **8**, 1345 (1996).
[20] K. Kunc, M. Balkanski, and M. Nusimovici, Phys. Status Solidi B **72**, 229 (1975).
[21] E. Molinari, S. Baroni, P. Giannozzi, and S. de Gironcoli, Phys. Rev. B **45**, 4280 (1992).
[22] R. Merlin, C. Colvard, M. V. Klein, H. Morcoç, A. Y. Cho, and A. C. Gossard, Appl. Phys. Lett. **36**, 43 (1980).
[23] S. Baroni, S. de Gironcoli, and P. Gianozzi, Phys. Rev. Lett. **65**, 84 (1990).
[24] J. Spitzer *et al.*, Solid State Commun. **84**, 275 (1992).
[25] V. G. Litovchenko, D. V. Korbutyak, S. G. Krylyuk, H. T. Grahn, and K. H. Ploog, in *Physics of Semiconductors: Proceedings of the 23rd International Conference*, edited by M. Scheffler and R. Zimmerman (World Scientific, Singpore, 1996), p. 859.